# Structure and Function of the Cytoskeleton of a *Dictyostelium* Myosin-defective Mutant

**Yoshio Fukui,* Arturo De Lozanne,‡ and James A. Spudich‡**

*Department of Cell, Molecular, and Structural Biology and Anatomy, Northwestern University Medical School, Chicago, Illinois 60611; and ‡Department of Cell Biology, Stanford University School of Medicine, Stanford, California 94305

***Abstract.*** To study the role of conventional myosin in nonmuscle cells, we determined the cytoskeletal organization and physiological responses of a *Dictyostelium* myosin-defective mutant. *Dictyostelium hmm* cells were created by insertional mutagenesis of the myosin heavy chain gene (De Lozanne, A., and J. A. Spudich. 1987. *Science (Wash. DC).* 236: 1086–1091). Western blot analysis using different mAbs confirms that *hmm* cells express a truncated myosin fragment of 140 kD (HMM-140 protein) instead of the normal 243-kD myosin heavy chain (MHC). Spontaneous revertants appear at a frequency $<4 \times 10^{-5}$, which synthesize normal myosin and are capable of forming thick filaments. In *hmm* cells, the HMM-140 protein is diffusely distributed in the cytoplasm, indicating that it cannot assemble into thick filaments. The actin distribution in these mutant cells appears similar to that of wild-type cells. However, there is a significant abnormality in the organization of cytoplasmic microtubules, which penetrate into lamellipodial regions. The microtubule networks consist of ~13 microtubules on average and their pattern is abnormal. Although *hmm* cells can form mitotic spindles, mitosis is not coordinated with normal furrow formation.

The *hmm* cells are clearly defective in the contractile events that lead to normal cytokinesis. The retraction of different regions of the cell can result in the occasional pinching off of part of the cell. This process is not coupled with formation of mitotic spindles. There is no specific accumulation of HMM-140 in such constrictions, whereas 73% of such cells show actin concentrated in these regions.

The mutant *hmm* cells are also deficient in capping of Con-A-bound surface receptors, but instead internalize this complex into the cytoplasm. The *hmm* cells display active phagocytosis of bacteria. Whereas actin is concentrated in the phagocytic cups, HMM-140 protein is not localized in these regions. cAMP, a chemoattractant that induces drastic rounding up and formation of surface blebs in wild type cells, does not induce rounding up in the *hmm* cells. A Triton-permeabilized cell model of the wild-type amebae contracts on reactivation with Mg-ATP, whereas a model of the *hmm* cell shows no detectable contraction. Our data demonstrate that the conventional myosin participates in the significant cortical motile activities of *Dictyostelium* cells, which include rounding up, constriction of cleavage furrows, capping surface receptors, and establishing cell polarity.

MYOSIN is the major mechanochemical transducer in muscle tissue, and believed to play essential roles in nonmuscle cell motility. It has been suggested that myosin is involved in cell locomotion (6, 7), cytokinesis (17, 34, 45, 56), phagocytosis (50), capping of surface receptors (4, 47), cytoplasmic streaming (46), and ameboid movement (20).

Nonmuscle myosin is similar to muscle myosin and composed of heavy and light chains. The biochemical properties of nonmuscle myosin have been extensively studied in *Dictyostelium discoideum* (1, 6, 7, 33, 51). The heavy chain is associated with one each of the regulatory (18-kD) and essential (16-kD) light chains (6, 7). Phosphorylation of the regulatory light chain enhances the actin-activated ATPase (1) and the ability of the myosin to move in vitro (26). The 243-kD heavy chain has at least two phosphorylation sites, which have been mapped to a 32-kD tail fragment (38). Phosphorylation of the heavy chain inhibits assembly of the filaments and leads to partial inactivation of the actin-activated ATPase (33). A similar property has been shown for myosin-II of *Acanthamoeba castellanii* (9, 28, 42, 43). The organization of *Dictyostelium* myosin into thick filaments and their localization in situ have been studied (14, 39, 44, 55, 56). The filaments are largely accumulated in the posterior cortex of migrating amoebae and organized to form the contractile ring during cytokinesis. Biochemical (1) and im-

Dr. De Lozanne's present address is Department of Molecular Genetics, University of Texas Southwestern Medical Center, 5323 Harry Hines Blvd., Dallas, TX 75235.

munofluorescence evidence (36, 55) showed that myosin is translocated to the cell cortex after stimulation with cAMP, the natural chemoattractant for these cells.

It has been shown that *Dictyostelium* has a single genomic copy of the myosin heavy chain gene (*mhc*A gene) (13, 15), which has been cloned and sequenced (15, 52). Disruption of the *Dictyostelium mhc*A gene was obtained by the integration of a transfected plasmid by homologous recombination (12). The transforming plasmid, pNEO-HMM-140, contained a 3.6-kb segment of the *mhc*A gene coding for a *Dictyostelium* myosin fragment equivalent to muscle heavy meromyosin (HMM).[1] As a result of the plasmid integration, the transformed cells, called *hmm* cells, expressed only the myosin fragment (HMM-140) coded for by the plasmid. Surprisingly, *Dictyostelium hmm* cells survive and display many forms of cell movement including chemotaxis. However, the *hmm* cells are defective in cytokinesis and cannot proceed through the developmental cycle. The same phenotype was obtained when *Dictyostelium* cells were transformed with a vector that synthesized myosin antisense RNA (32). These transformed cells accumulate <5% of the normal myosin levels. Given that both cell types, one with a truncated form of myosin and the other with a reduced amount of myosin, still express substantial motile activity, raises the fundamental question of what is the role of myosin in nonmuscle cells (27, 48). The possibility that the motility of these cells is due to the presence of low amounts of normal myosin in those cells (12, 32) has been ruled out by a recent study on myosin null mutants (35).

Recent studies have characterized further the effect of the absence of myosin in *Dictyostelium* cells. Although *hmm* cells are able to move across a surface, they do so at reduced velocity (2.3 μm/min) compared with wild-type cells (5.9 μm/min) (53). The organization of the HMM-140 protein in the cytoplasm and the possible changes in the organization of actin and microtubules in *hmm* cells have remained unsolved. This study was performed to assess the function of the conventional myosin in *Dictyostelium* by determining the organization of the HMM-140 protein, actin, and microtubules in *hmm* cells. These data show that the conventional myosin is significantly involved in organization and function of the cortical cytoskeleton.

## Materials and Methods

### Cell Culture

*Dictyostelium hmm* cells were cultured in plastic Petri dishes containing HL-5 medium (8) supplemented with G418 (Geneticin; Gibco Laboratories, Grand Island, NY) at 10 μg/ml. At stationary phase, cells were transferred to fresh medium. Every 4 wk, the original culture was recovered by thawing the cells frozen in HL-5 medium containing 5% DMSO. The parental strain, Ax4, was cultured in the same manner but in medium without G418. The wild type strain, NC4, was cultured in association with *Escherichia coli* (B/r) on nutrient agar plates containing 0.2% lactose, 0.2% Bacto peptone, and 2% Bacto agar (2). The aggregation-competent cells were prepared by washing the late-exponential phase cells with Bonner's salt solution (10 mM NaCl, 10 mM KCl, 3 mM $CaCl_2$) and incubated for 2–6 h on 2% agar plates containing 15 mM Na/K-phosphate (pH 6.5).

1. *Abbreviations used in this paper*: HMM, heavy meromyosin; MHC, myosin heavy chain.

### Antibodies

Mouse mAbs against *Dictyostelium* myosin were used. My-3 (41) binds to the HMM region and My-1 (41) binds to the LMM (light meromyosin) region. A mouse mAb against native chick brain alpha-tubulin (DM1α) was a gift from Dr. Steven H. Blose (Cold Spring Harbor Laboratory) (31). The ascites fluid was diluted to 1:500, and purified IgG was used at a concentration of 10 μg/ml for the immunofluorescence. FITC-goat anti-mouse IgG (Southern Biotechnology Associates, Inc., Birmingham, AL) and TMRITC-goat anti-mouse IgG (Sigma Chemical Co., St. Louis, MO) was used at 1:25 dilution.

### Western Blot

Cell lysates were made by dissolving $10^7$ cells with 1 ml of hot SDS sample buffer containing 2% SDS, 100 mM DTT, 10 mM PMSF, and 5 mM TLCK. Electrophoresis was run on a 7.5% polyacrylamide gel using a Mini-Gel apparatus (Bio-Rad Laboratories, Richmond, CA), and a transblot was made using a Mini-Transblot system (Bio-Rad Laboratories) in a buffer containing 25 mM Tris, 192 mM glycine, 20% methanol, and 0.1% SDS (pH 8.3) at 30 V for 12 h. After blocking with 1% gelatin (type I, Sigma Chemical Co.) and 1% BSA (type V, Sigma Chemical Co.) for 30 min, the nitrocellulose paper was incubated with My-1 (10 μg/ml) or My-3 (1:500 ascites fluid) for 2 h. After washing with Tris-buffered saline containing Tween-20 (20 mM Tris, 150 mM NaCl, pH 7.5, 0.05% Tween-20), the samples were incubated in 1:2500 HRP-labeled goat anti-mouse immunoglobulin (Bio-Rad Laboratories) for 1 h. The nitrocellulose paper was processed using a HRP Color Development System (Bio-Rad Laboratories) for 20 min.

### Immunofluorescence

Cells were prepared by the agar-overlay technique (22, 23). Briefly, cells were overlaid with a thin agarose sheet (0.15 mm thick, 8 × 8 mm wide, made of 2% agarose dissolved in Bonner's salt solution). Cells grow well under these conditions and behave normally. For indirect immunofluorescence for myosin and tubulin, the samples were fixed for 5 min in −15°C methanol containing formalin at 1%. For staining with rhodamine-phalloidin (Molecular Probes, Inc., Eugene, OR) for F-actin, the samples were fixed with −15°C acetone for 3 min. After fixation, the agarose sheet was removed from the coverslip during a 10-min wash in PBS (137 mM NaCl, 2.7 mM KCl, 1.5 mM $KH_2PO_4$, 8.0 mM $Na_2HPO_4$, pH 7.4). The samples were incubated with the primary antibody for 30 min at 37°C, washed in PBS for 10 min, and reincubated with secondary antibody. For double staining, they were incubated with 3.3 μg/ml rhodamine-phalloidin in PBS for 20 min at 37°C. For triple staining, DAPI (4',6'-diamidino 2-phenylindole, Sigma D-1388; final concentration 0.2 μg/ml) was mixed with rhodamine-phalloidin. After washing, the samples were mounted with a mixture of glycerol and polyvinyl alcohol containing DABCO (1,4-diazabicyclo[2.2.2]-octane, Aldrich Chemical Co., Milwaukee, WI) (22).

### Image Recording and Quantitation

Fluorescence micrography was done using a Zeiss Photomicroscope-III (Carl Zeiss, Inc., Thornwood, NY) attached with a plan-Neofluar 40X (NA 0.9), plan apo 63X (NA 1.4), or Neofluar 100X (NA 1.3) objective lens. The filter systems used were UV G365 (487701), BL 450-490SB (487710), and GR H546 (487715). Micrographs were taken with a camera factor of 4 using Kodak Tmax-400 film (Eastman Kodak Co., Rochester, NY) and developed with Diafine (Acufine Inc., Chicago, IL). The quantitation was made by a through-focus observation using the plan apo 63X objective.

### Video Microscopy

The video microscopy was performed using a Nikon TMD inverted microscope attached with a 40X DIC objective (NA 0.55). The image was recorded in real time through a DAGE-MTI 67M camera equipped with a newvicon tube using a Sony VO-5800H 3/4" video cassette recorder. The original tape was image-processed using a video image processor (model 794; Hughes, Dedham, MA) with the frame averaging function, and the time-lapse analysis was made by dubbing to a 1/2-in. tape using a Gyyr model TLC 2001 time-lapse video cassette recorder. The freeze images were photographed using a Nikon N-2000 camera loaded with Kodak Panatomic-X film and developed with Kodak Microdol-X.

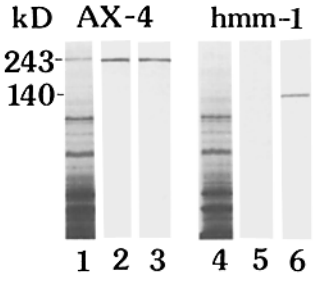


*Figure 1.* Western blot of AX4 (lanes *1–3*) and *hmm* (lanes *4–6*) cell lysates. The cell lysates equivalent to $10^5$ cells were subjected to electrophoresis. Lanes *1* and *4*: SDS-polyacrylamide gels stained with Coomassie brilliant blue. Lanes *2* and *5*: immunostain with My-1 (anti-LMM). Lanes *3* and *6*: immunostain with My-3 (anti-S2). Whereas the parental AX4 cells contain normal myosin heavy chain with 243 kD molecular mass, *hmm* cells only express a 140-kD protein.

### *Phagocytosis of Bacteria*

*E. coli* (B/r) was cultured for 2 d, washed three times by centrifugation (4,000 rpm, 5 min) and suspended in Bonner's salt solution at $10^{11}$ cells/ml. Nine parts of *hmm* cells ($5 \times 10^6$ cell/ml) and one part of the bacteria ($5 \times 10^9$ cells/ml) were mixed, prepared for the agar-overlay method, and incubated for 60 min at 22°C. The samples were fixed for the staining for myosin and actin.

### *Capping of Con-A Receptors*

A 200-μl aliquot of FITC-Con-A (1 mg/ml) (C-7642, Sigma Chemical Co.) was dialyzed against Con-A buffer containing 15 mM Na/K-phosphate (pH 6.5), 1 mM $CaCl_2$, and 2 mM $MgSO_4$ for 6 h at 4°C, and diluted to 2 ml with the same buffer. A 200-μl aliquot of diluted FITC-Con-A was spun down at 13,000 rpm for 2 min, and the supernatant was mixed with 86 μl of the cell suspension ($5 \times 10^6$ cells/ml). The suspension was incubated in a small, round bottom test tube at 22°C, and occasionally monitored under a Zeiss Photomicroscope-III. At 10, 15, 20, 30, and 40 min of incubation, 80 μl of aliquot of the sample was fixed for immunofluorescence by mixing 20 μl of 10% formalin in PBS. After 5 min, the cells were washed three times with Bonner's solution by centrifugation (1400 rpm, 1.5 min) and processed for the agar-overlay technique for immunofluorescence staining.

### *Stimulation with cAMP*

An aliquot of cell suspension was dropped on a coverslip and overlaid with an agarose sheet ("agar-overlay" method). The excess solution was removed, and the sample was incubated in a moist chamber for several hours. Etched grid coverslips (Bellco Biotechnology, Vineland, NJ) were used for relocating the recorded cells after immunofluorescence stain. The samples were occasionally monitored under a Nikon Optiphot microscope equipped with a 40X DLL phase-contrast lens (NA 0.55). When a sign of the initiation of aggregation was observed, the coverslip was placed on a stage of the TMD microscope and the video microscopy was started. An aliquot (2.5 μl) of $10^{-6}$ M cAMP (A-6885, Sigma Chemical Co.) in Bonner's solution was applied to the sample using a microcapillary with 5 μl capacity connected to a screwed microsyringe. The capillary was manipulated using a Narishige MO 104M-R micromanipulator (Narishige Scientific Instrument Laboratories, Tokyo, Japan). The solution was perfused by blotting off the solution with a thin piece of filter paper using a Narishige MN-100N manipulator.

### *Reactivation with ATP*

The agar-overlaid cells were permeabilized for 5 minutes on ice with 5 μl of P buffer made of 10 mM Hepes (pH 7.6), 50 mM KCl, 1 mM $MgCl_2$, 10 mM EGTA, 1 mM DTT, 50 μg/ml leupeptin (L-2884, Sigma Chemical Co.) containing 0.5% Triton X-100 (Sigma Chemical Co.). The sample was placed on a Nikon TMD microscope stage for video microscopy. A 5-μl aliquot of the reactivation buffer (A solution) containing 1 mM ATP (A-3377, Sigma Chemical Co.) in the P buffer was applied in the same way as the application of cAMP. Alternatively, the sample was presaturated with A solution on a microscope stage, then a 1:1 mixture of A solution and P buffer was added. The final concentrations of ATP and Triton X-100 were 1 mM and 0.5%, respectively. The two methods gave identical results but the latter method was more reproducible. The experiment was repeated at least 10 times for all of the strains. The control experiments were done using vanadium-free ADP (A-6521, Sigma Chemical Co.) and CTP (C-7381, Sigma Chemical Co.).

## *Results*

### *Immunological Characterization of hmm Cells*

The *hmm* cells contain between 5 and 10 copies of the transforming plasmid pNEO-HMM-140 integrated as a tandem array into the *mhc*A gene (12). As a consequence of this integration, the cells transcribe an mRNA species of ~4.3 kb (corresponding to the HMM-140 mRNA) instead of the 7-kb MHC mRNA. Since the HMM-140 protein expressed in the *hmm* cells lacks 892 amino acid residues from the COOH terminus of the MHC molecule, it is possible to distinguish between transformed and revertant cells by the use of an antibody (My-1) which binds within the 892 amino acid COOH-terminal segment.

We have used two different monoclonal antibodies directed against *Dictyostelium* myosin, My-1 and My-3; the epitope for My-3 is contained within HMM-140 (41). Western blot analyses showed that whereas the 243-kD MHC of the paren-

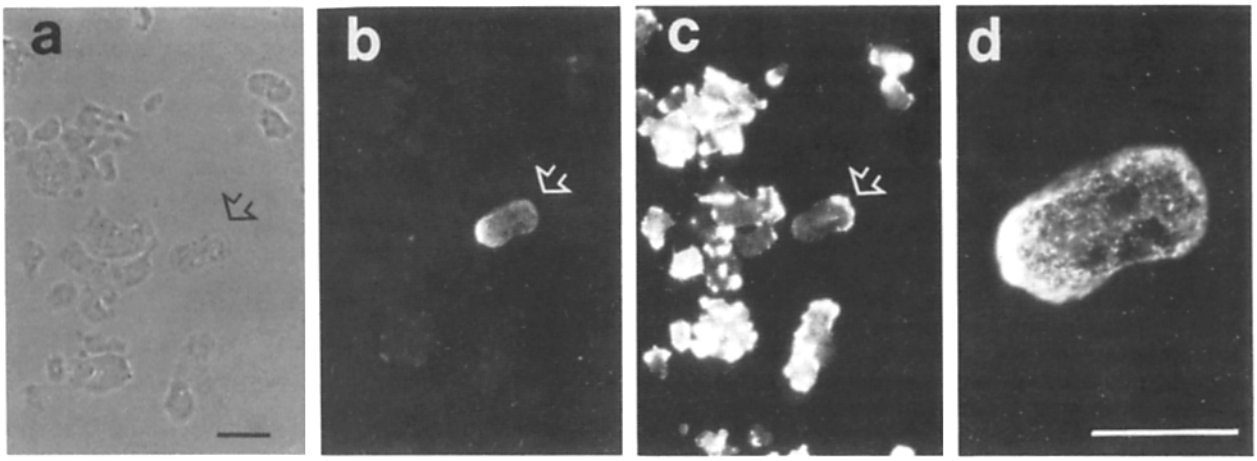


*Figure 2.* Fluorescence staining of the *hmm* cells with My-1 and rhodamine-phalloidin to identify spontaneous revertants. The revertants, which express the LMM region of the myosin tail (*b*) and contain myosin filaments (*d*), appear at a frequency $<4 \times 10^{-5}$. *Arrow* in *c*, heavy staining of F-actin in the anterior pseudopodium. Bar, 10 μm. (*a–c*) ×700; (*d*) ×2,000.

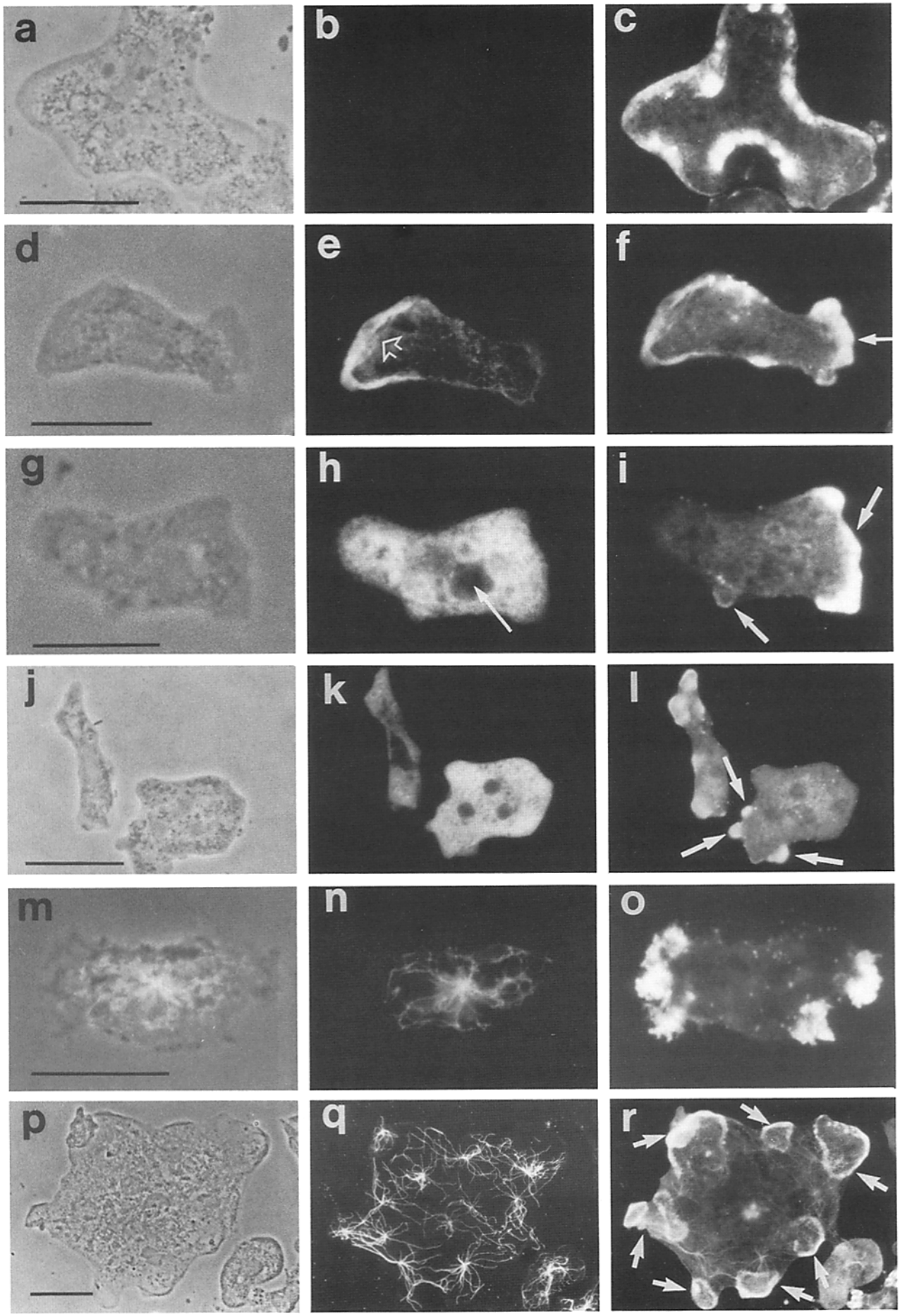
a
b
c
d
e
f
g
h
i
j
k
l
m
n
o
p
q
r

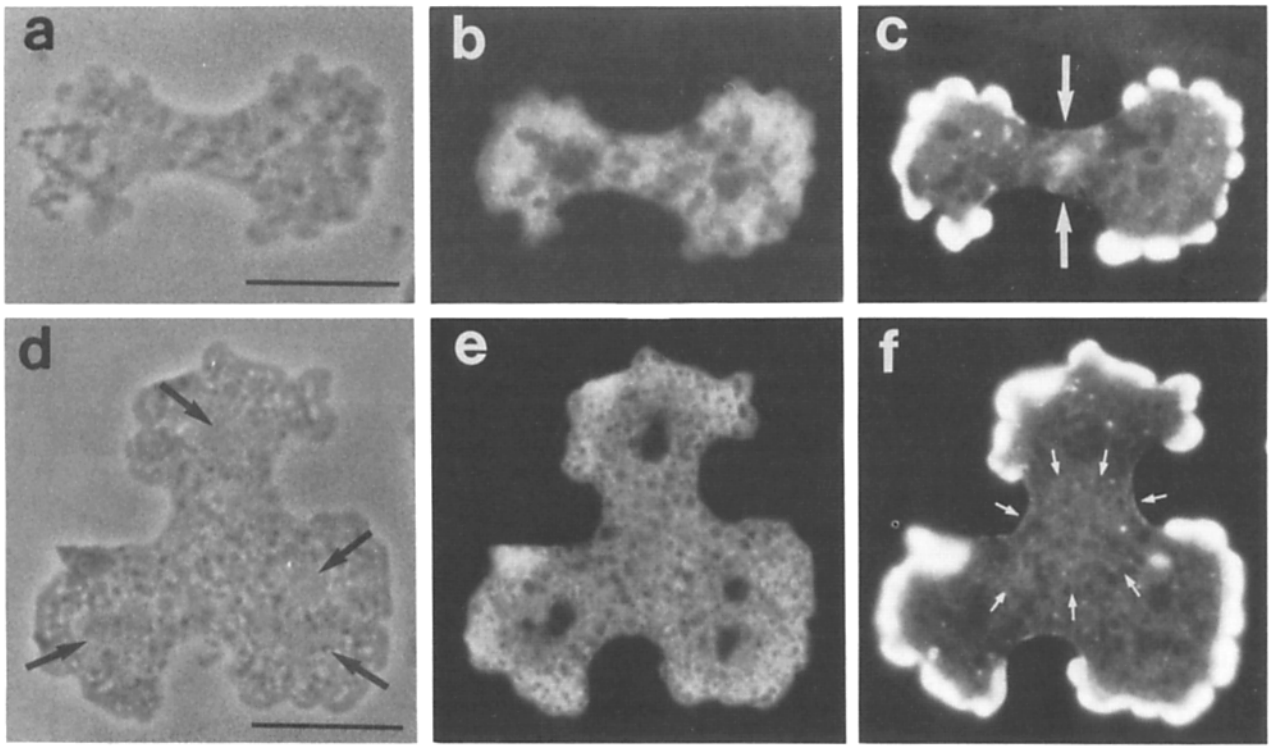


*Figure 4.* Fluorescence microscopy of *hmm* cells stained with My-3 (*b* and *e*) and rhodamine-phalloidin (*c* and *f*) during traction-mediated cytofission. (*a–c*) A binucleate *hmm* cell with a "pseudo-cleavage furrow". *Arrows* in *c*: pseudo-cleavage furrow. (*d–f*) A multinucleated *hmm* cell forming multipolar pseudo-cleavage furrows. *Arrows* in *f*: accumulation of F-actin in the central region of the cell body. Bar, 10 μm. ×2,000.

tal Ax4 strain was recognized by both mAbs (Fig. 1, lanes *2* and *3*), and 140-kD HMM protein of the *hmm* cells was only recognized by My-3 (Fig. 1, lane *6*). There was no detectable MHC in lysates of *hmm* cells by Coomassie staining (Fig. 1, lane *4*), or by immunoblot staining with My-1 (Fig. 1, lane *5*) under conditions that can detect MHC in extracts from as few as 100 cells (12).

The lack of normal MHC in individual *hmm* cells was demonstrated by the absence of immunofluorescence staining using My-1 (Fig. 2). Cells that showed a positive staining with My-1 appeared, at a frequency $<4 \times 10^{-5}$ (Fig. 2 *b*). These cells appear to represent revertant cells. At a higher magnification, the staining pattern of these revertant cells showed the typical pattern for the myosin filaments found in wild-type cells (55, 56) (Fig. 2 *d*). The actin localization showed that this revertant cell was well polarized and formed the anterior pseudopodium which was filled with F-actin (Fig. 2 *c*, *arrow*). The accumulation of myosin in the posterior cortex (Fig. 2 *d*) was similar to that of the wild type. The low frequency of reversion events found in our preparations indicates that the cells identified throughout this study were the *hmm* cells and not revertant cells, at least with a probability $>2.5 \times 10^{4}$:1.

### *Cytoskeletal Organization*

When *hmm* cells were stained with mAb that binds only to full-length myosin (My-1), there was no staining in the cell (Fig. 3 *b*). As a control, the parental Ax4 cells were stained with My-1 (Fig. 3 *e*). The conventional myosin formed filaments and most of the myosin was accumulated in the posterior cortex. In Ax4 cells, F-actin was localized in the posterior cortex as well as in the anterior pseudopodium (Fig. 3 *f*, *arrow*). This actomyosin organization was identical to that of the wild-type NC4 as previously studied (20, 56).

When *hmm* cells were stained with My-3 for the HMM-140 protein, the cell showed only a mottled fluorescence in the cytoplasm and no specific accumulation was observed (Fig. 3 *h*). The multinucleated cells also displayed only diffuse fluorescence (Fig. 3 *k*). The distribution of F-actin looked normal; there was an extensive accumulation in pseu-

*Figure 3.* Fluorescence microscopy of myosin and actin in AX4 and *hmm* cells as shown by staining with mAbs and rhodamine-phalloidin. (*a–c*) Control staining of *hmm* cells with My-1 for LMM (*b*) and rhodamine-phalloidin (*c*) for F-actin. (*d–f*) Control staining of the parental AX4 with My-1 (*e*) and rhodamine-phalloidin (*f*). *Arrow* in *e*: posterior cortex. *Arrow* in *f*: anterior pseudopodium. (*g–i*) A representative uninuclear *hmm* cell stained with My-3 (*h*) and rhodamine-phalloidin (*i*). *Arrow* in *h*: nucleus. *Arrows* in *i*: pseudopodia. (*j–l*) Multinucleated *hmm* cells stained with My-3 (*k*) and rhodamine-phalloidin (*l*). *Arrows* in *l*: pseudopodia. (*m–o*) Double staining of a wild-type AX4 cell with DM1α (*n*) and rhodamine-phalloidin (*o*). A phase-contrast micrograph was double-exposed with the FITC image showing the zone of microtubules (*m*). (*p–r*) Double staining of a multinucleated *hmm* cell stained with DM1α (*q*) and rhodamine-phalloidin (*r*). *Arrows* in *r*: the regions where microtubules are superimposed with F-actin. Bar, 10 μm. (*a–i*) ×2,200; (*j–l*) ×1,800; (*m–o*) ×2,200; (*p–r*) ×1,200.

dopodia and lamellipodia (Fig. 3, *i* and *l*, *arrows*). However, compared with wild-type cells where the microtubules are excluded from such actin-rich regions (Fig. 3, *m–o*), in *hmm* cells, microtubules were superimposed with these regions (Fig. 3, *p–r*). This result demonstrated that the cortical cytoskeleton was altered by such a way that allowed the microtubules to penetrate into the microfilament network.

It was reported that *hmm* cells do not undergo cytokinesis during a 48-h observation period (12), but they instead occasionally "pinch off" fragments of cytoplasm. The present video-microscopic studies showed that *hmm* cells, on a substratum, periodically displayed a distinctive morphology that to some extent mimicked the cleavage furrow formed by the wild-type during cytokinesis. We refer to this constriction as a "pseudo-cleavage furrow", the term used by Knecht and Loomis (32). However, unlike normal cytokinesis, this shape change clearly requires forces associated with cell adhesion to a surface; *hmm* cells filmed in suspension do not show this shape change during mitosis (Spudich, J. A., and S. J. Kron, unpublished observations). These workers have coined the term "traction-mediated cytofission" to refer to shape changes that result from adhesion forces that can lead to cell fragmentation. My-3 staining in cells showing a pseudo-cleavage furrow revealed that the protein HMM-140 was only diffusely

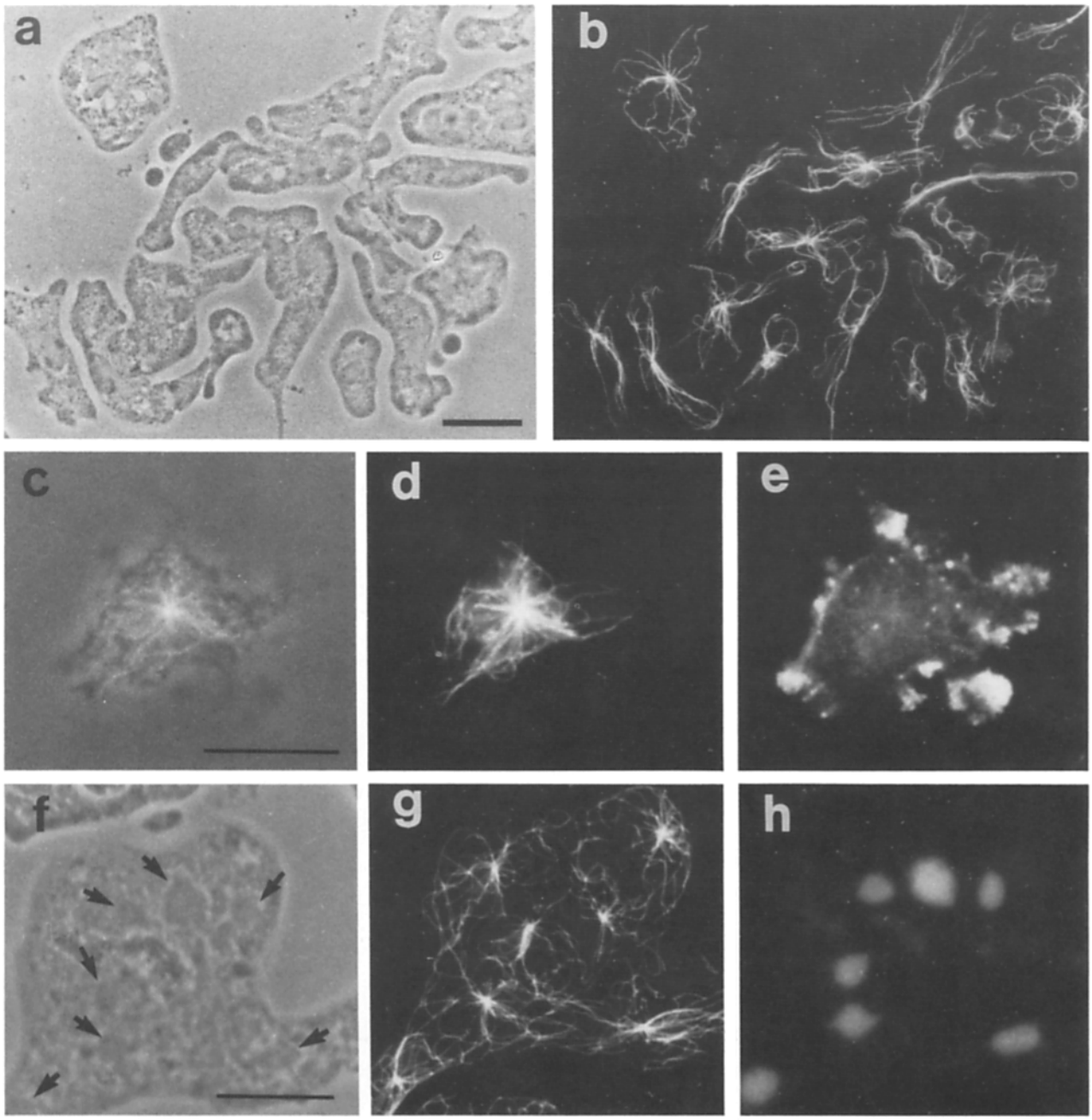


*Figure 5.* Microtubule organization of *hmm* cells as shown by immunofluorescence staining with DM1α. (*a* and *b*) Low-magnification micrographs of *hmm* cells stained with DM1α (*b*) showing a variation of microtubule organization and numbers (15 ± 7 microtubules per network). (*c–e*) A uninuclear cell containing a single microtubule network as shown by double-exposed (*c*) and fluorescence micrographs stained with DM1a (*d*) and rhodamine-phalloidin (*e*). (*f–h*) A multinucleated cell containing at least seven microtubule networks as demonstrated by staining with DM1a (*g*) and DAPI (*h*). Bar, 10 μm. (*a*, *b*) ×1,200; (*e*) ×2,100; (*f–h*) ×1,800.

distributed in the cytoplasm (Fig. 4 *b*). In contrast, actin was localized in the polar pseudopodia (Fig. 4 *c*). In 73% of such cells ($n$ = 159), F-actin was also localized in the pseudo-cleavage furrow (Fig. 4 *c*, *arrows*). Note that cells of this type contained well-established interphase microtubule networks rather than mitotic spindles (Fig. 7, *j–l*). The multinucleated *hmm* cells also formed pseudo-cleavage furrows (Fig. 4 *d*). The staining with My-3 showed the same mottled fluorescence (Fig. 4 *e*), and the localization of F-actin in the pseudopodia was identical to that of the binucleate *hmm* cells. Frequently, F-actin was also localized in the central region of the cytoplasm (Fig. 4 *f*, *arrows*).

The *hmm* cells extend pseudopodia, lamellipodia, and filopodia in random directions and the cells appear to lose their morphological polarity. As cell polarity is tightly related to microtubule organization (30, 31, 37, 54), we studied the organization of microtubules in *hmm* cells by immunofluorescence. Compared with a relatively uniform number of microtubules in wild-type cells (34.2 per cell in reference 29), there was a wide variation in *hmm* cells (Fig. 5 *b*). Many *hmm* cells had multiple numbers of microtubule networks, and each network had, on the average, 13 ± 4 ($n$ = 90) microtubules. Two representative *hmm* cells are shown at high magnification. One cell (Fig. 5 *c*) appeared to be uninucleate, and contained ~50–60 microtubules (Fig. 5 *d*). The same cell formed many surface projections which contained F-actin (Fig. 5 *e*). The other cell shown in Fig. 5 *f* was multinucleated, and contained seven nuclei as shown by DAPI staining (Fig. 5 *h*; also see *arrows* in 5 *f*). Each nucleus of this multinucleated cell was usually associated with single microtubule networks (Fig. 5 *g*).

### *Physiological Properties*

It has been previously shown that in wild-type cells actin is accumulated at cell–cell adhesion sites, whereas myosin is localized at the opposite side of the cell cortex (56). In this study, we found that, in *hmm* cells, actin is accumulated in the cell–cell adhesion sites (Fig. 6 *c*). In contrast, HMM-140 protein was distributed diffusely in the cytoplasm and apparently excluded from the region near the cell-cell contact site (Fig. 6 *b*).

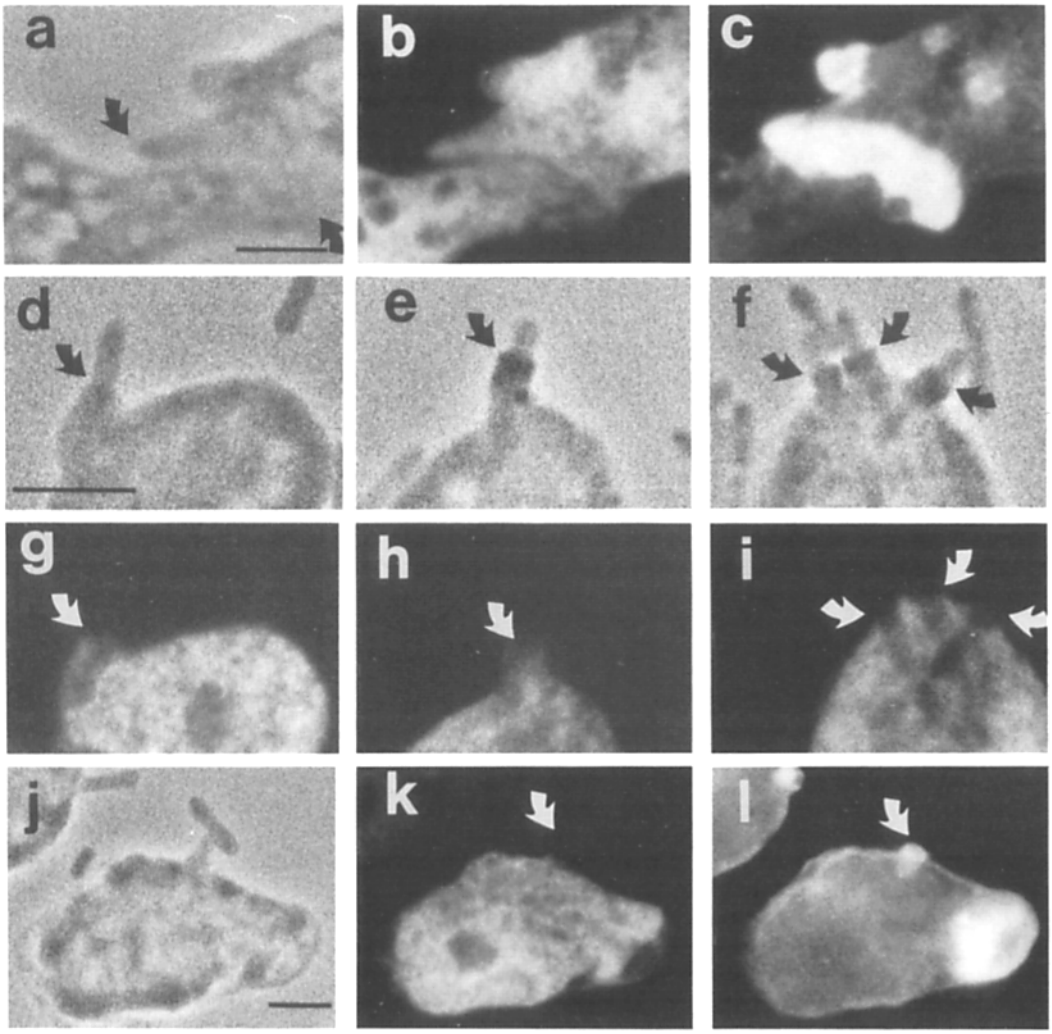


*Figure 6.* Cell–cell adhesion and phagocytosis of *hmm* cells. (*a–c*) Two *hmm* cells contacting each other at lamellipodia (*arrows*) showing the distribution of HMM-140 protein as stained with My-3 (*b*) and F-actin as stained with rhodamine-phalloidin (*c*). (*d–f*) Examples of phagocytic cups of *hmm* cells engulfing *E. coli*; arrows indicate the tip of phagocytic cup. (*g–i*) Fluorescence micrographs stained with MY-3. (*j–l*) A phase-contrast micrograph (*j*) and double-staining fluorescence micrographs stained with My-3 (*k*) and rhodamine-phalloidin (*l*). Bar, 2 μm. (*a–c*) ×6,000; (*d–i*) ×8,000; (*j–l*) ×4,000.

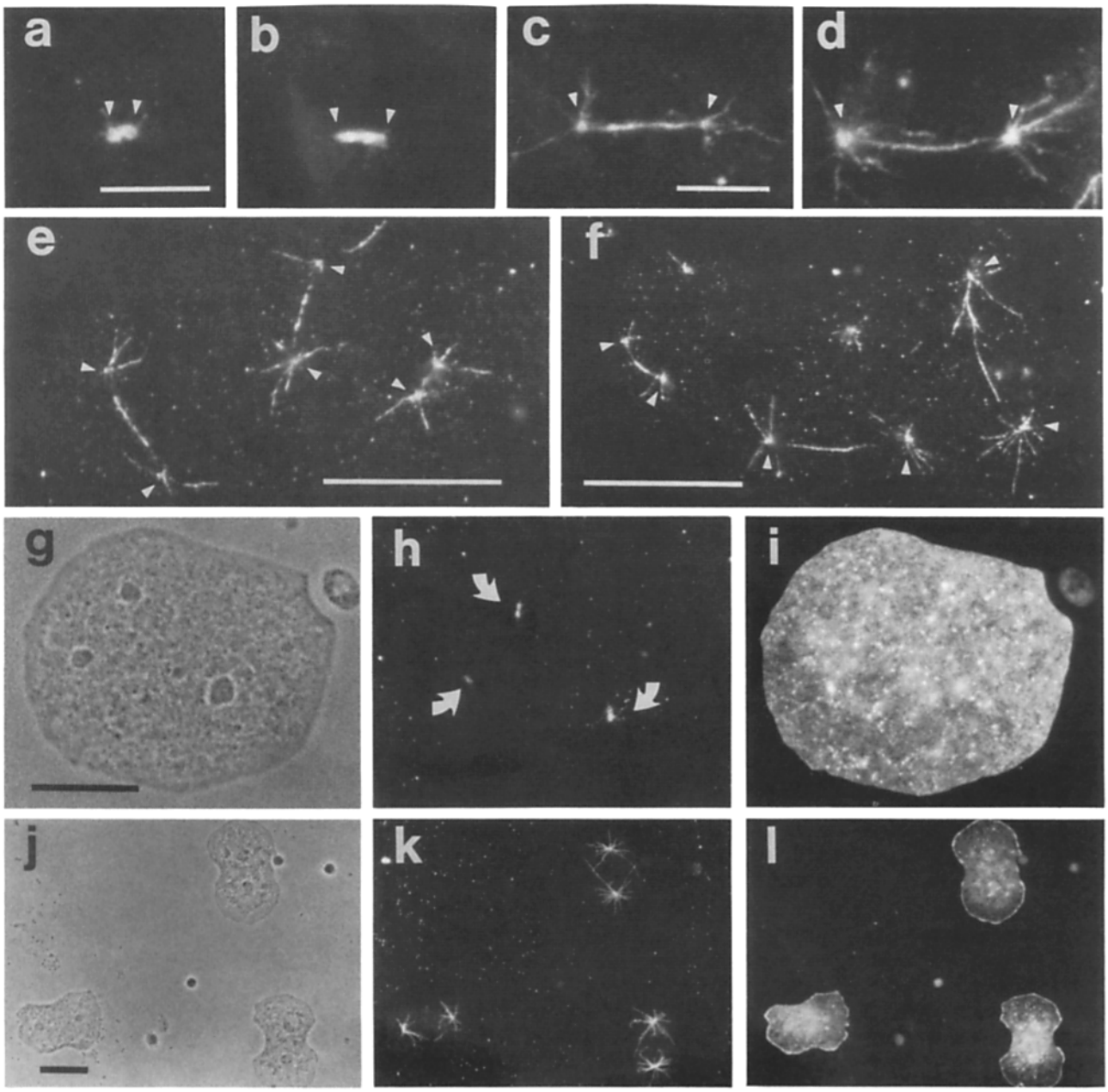


*Figure 7.* Mitosis and traction-mediated cytofission of *hmm* cells as shown by fluorescence staining with DM1α and rhodamine-phalloidin. (*a–d*) Examples of mitotic spindles representing prophase (*a*), metaphase (*b*), anaphase-B (*c*), and telophase (*d*). (*Arrowheads*) Spindle pole bodies. (*e* and *f*) Multinucleated cells performing synchronous mitosis in anaphase-B (*e*) and telophase (*f*). (*g–i*) A trinucleated cell including metaphase spindles (*h*, *arrows*) showing the dissociation of actin from the cortex (*i*). (*j–l*) Traction-mediated cytofission of *hmm* cells. Note prominent interphase microtubules (*k*), and actin localization in the pseudo-cleavage furrow (*l*). Bars, (*a–f*) 5 μm; (*g–l*) 10 μm. (*a* and *b*) ×3,400; (*c* and *d*) ×2,800; (*e*) ×5,400; (*f*) ×4,800, (*g–i*) ×1,600; (*j–l*) ×700.

The *hmm* cells internalized *E. coli* by forming apparently normal phagocytic cups (Fig. 6, *d–f*). Staining of the cells with My-3 showed that HMM-140 protein was not localized in such regions (Fig. 6, *g–i*). In contrast, the phagocytic cups contained a large amount of F-actin as shown by the double staining micrographs (Fig. 6, *j–l*, *arrow*).

The possible role of myosin during mitosis has been debated for many years. Because the disruption of the *mhc*A gene gives rise to a population of multinucleated cells, we were interested to study whether the multinucleation results from normal mitosis (30) or from abnormal nuclear division (18). We found that the *hmm* cells were capable of forming spindles. Fig. 7 shows examples of *hmm* cells with prophase, metaphase, anaphase, and telophase spindles (Fig. 7, *a*, *b*, *c*, and *d*, respectively), according to the criteria established for the wild-type cells (29). Multinucleated cells showed synchronous mitotic figures (Fig. 7, *e* and *f* for anaphase-B and telophase, respectively). As in the wild-type cells (30), actin showed extensive cytoplasmic stain during mitosis, and the cortical staining for actin decreased (Fig. 7, *g–i*). It

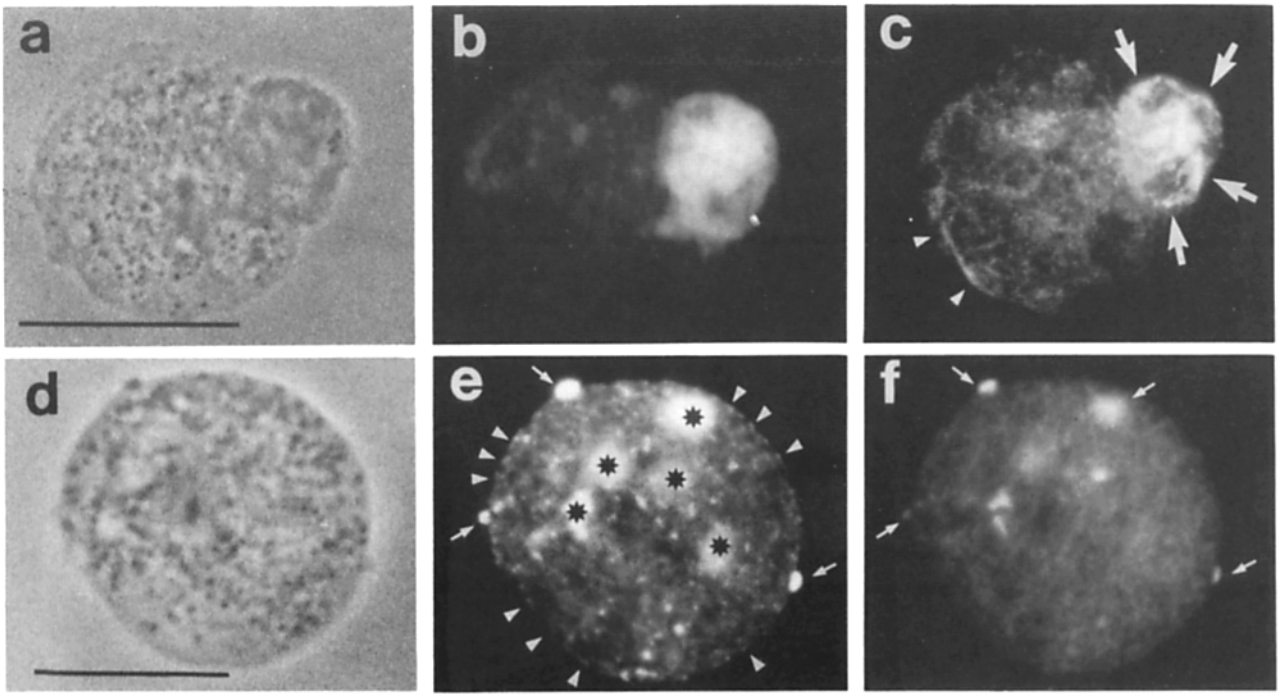


*Figure 8.* Phase-contrast and fluorescence micrographs of AX4 and *hmm* cells after stimulation with FITC-Con-A. (*a–c*) A parental AX4 cell after 15 min incubation with FITC-Con-A. (*b*) FITC-Con-A. (*c*) myosin localization as stained with My-3. (*Arrows*) Myosin fibrils under the cap. (*Arrowheads*) A linear array of myosin along the cortex. (*d–f*) *hmm* cells incubated for 40 min in the presence of FITC-Con-A. (*e*) FITC-Con-A. (*Arrows*) Aggregates of FITC-Con-A. (*Arrowheads*) patches. (*Asterisks*) internalized FITC-Con-A aggregates. (*f*) HMM-140 protein as stained with My-3. Punctate fluorescence in *f* (*arrows*) was caused by the leak of immense FITC signal into the rhodamine pass and does not show the true localization of HMM-140. Bar, 10 μm. (*a–c*) ×3,000; (*d–f*) ×2,500.

should be pointed out, however, that mitosis was not coupled with cytokinesis, and cytofission occurred when cells contained obvious interphase microtubule networks (Fig. 7, *j–l*).

It has been demonstrated that myosin as well as actin localizes below Con-A patches and moves with the patches into the Con-A cap (4). In this study, we stimulated the cells with FITC-labeled Con-A. After 10–15 min of incubation with Con-A, 20–30% of AX4 cells (Fig. 8, *a–c*) and >90% of NC4 cells showed capping (data not shown). The degree of the myosin localization in capped AX4 was variable with occasional presence of a fibrous array of myosin-containing structure in the cortex as well as in the capping region (Fig. 8 *c*, *arrows*). In marked contrast, *hmm* cells did not show any sign of capping. Instead, the mutant initiated extensive internalization of FITC-Con-A after 15–20 min of incubation (Fig. 8 *e*). There was a punctate array of small patches on the surface (Fig. 8 *e*, *small arrows*). HMM-140 protein was only diffusely present in the cytoplasm (Fig. 8 *f*). After 40 min, most of the FITC-Con-A was endocytosed and moved into the endoplasm (Fig. 8 *e*, *asterisks*). In experiments complementary to those described here, Pasternak, Spudich, and Elson (40), showed that *Dictyostelium* cells that lack the entire myosin heavy chain fail to cap surface receptors and to develop the normal increase in cortical tension associated with capping. Our experiments show that the tail portion of the myosin molecule, which is involved in thick filament formation, is essential for the capping process.

### *Contractile Properties*

cAMP is a chemoattractant for *Dictyostelium* (2, 3, 5), and induces drastic cell shape changes called "cringing" (24, 25). It has been shown that myosin filaments change their distribution during the cringing response (36, 55). It was shown that the parental AX4 cells rounded in 30 s in response to $10^{-6}$ M cAMP, and produced surface blebs, confirming our previous study (36). The *hmm* cells failed to round up in response to cAMP. They did, however, respond by producing surface blebs, but their response was slower (30–60 s) (Fig. 9, *a* and *b*). After 1 min, *hmm* cells looked irregular because they produced many surface blebs. We found that actin was localized in the newly formed blebs (Fig. 9 *e*, *arrows*), but there was no specific accumulation of the HMM-140 protein (Fig. 9 *d*). When a cell aggregate of *hmm* cells was stimulated, the cells responded in the same manner. Observation of such aggregates for 10–15 min after the initial stimulation showed that the cells started to migrate with random orientation, and eventually the aggregate dissociated (Fig. 9, *f–i*). The results demonstrated that the *hmm* cells respond to cAMP by forming surface blebs and reorienting their migration vectors but do not show obvious rounding up of the cell body.

Cytoskeletons of the parental AX4 cells showed a drastic contraction in 15–30 s after addition of Mg-ATP (Fig. 10, *a–c*). In control experiments, no contraction was observed after addition of ADP or CTP (data not shown). In contrast, cytoskeletons of *hmm* cells did not show any apparent contraction of the entire cortical cytoskeleton after addition of Mg-ATP (Fig. 10, *d–f*). The permeabilization of the membrane system only resulted in the breakdown of vacuoles and mitochondria, and these changes were followed by the total

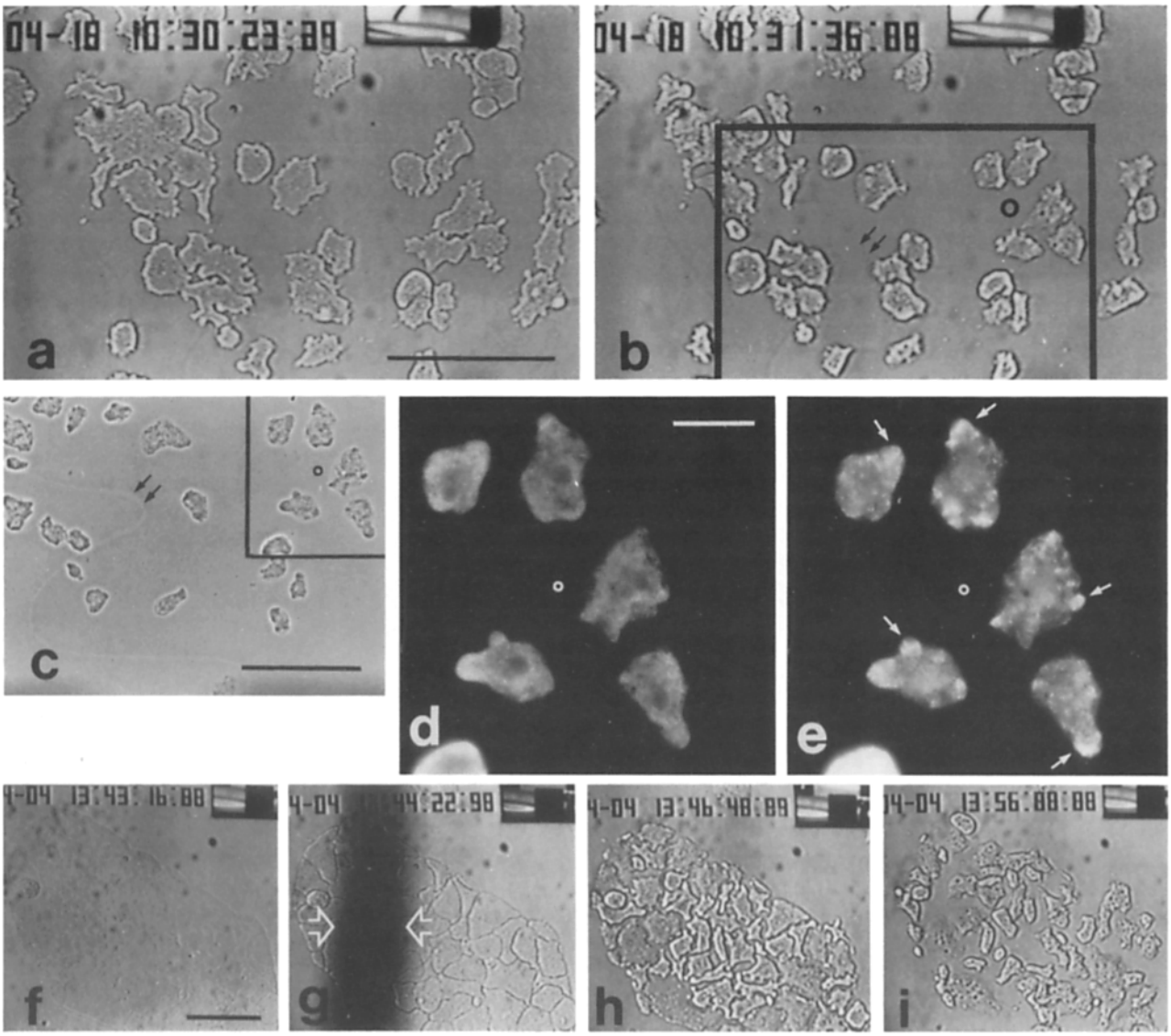


*Figure 9.* Response of *hmm* cells to cAMP. (*a* and *b*) Video microscopy of *hmm* cells before (*a*) and 45 s after (*b*) stimulation with $10^{-6}$ M cAMP. At ~1 min, the cells were fixed (*c*) and stained with My-3 (*d*) and rhodamine-phalloidin (*e*). The whole fields of *d* and *e* correspond to marked areas in *b* and *c*. *Circles* in *b* and *c* correspond to *circles* in *d* and *e*. *Paired arrows* in *b* and *c* etched line on a coverslip. *Arrows* in *e*, blebs induced with cAMP. (*f–i*) Sequential video frames showing the dissociation of a cell aggregate after the cAMP stimulation. (*f*) 66 s before the stimulation. The dark line in *g* (*arrows*): wave of cAMP solution crossing the field (0 s). (*h*) 146 s, and *i*: 11 min, 37 s after the stimulation. (*a*, *c*, and *f*) 50 μm; (*d*) 10 μm. Magnifications: (*a* and *b*) ×480; (*c*) ×340; (*d* and *e*) ×1,200; (*f–i*) ×220.

lysis of the cell model after several minutes of incubation (Fig. 10 *f*).

## Discussion

### Cytoskeleton of hmm Cells

This study demonstrated that HMM-140 protein is diffusely localized and does not form any structural organization at the resolution of 200 nm, which is the average thickness of the conventional myosin filaments as shown previously (55). Actin localization appeared normal in *hmm* cells during spreading, migration, cell-cell adhesion and phagocytosis. It is important to note, however, that the microtubules frequently penetrated into cortical lamellipodial regions where F-actin was accumulated. This suggests that the absence of conventional myosin results in the weak organization of cortical microfilament architecture, which allows the invasion of microtubules into these regions.

We also found a significant abnormality in the number of microtubules and the multiplicity of the networks. As previously shown, the multinucleated giant cells induced with microtubule inhibitors showed a similar variation in the microtubule system (31). This coincidence observed in two different systems suggests that these features of microtubule abnormality might be an indirect effect of multinucleation rather than a direct effect of lack of conventional myosin.

### Motility and Cell Division of hmm Cells

It appears important that *hmm* cells showed little behavioral

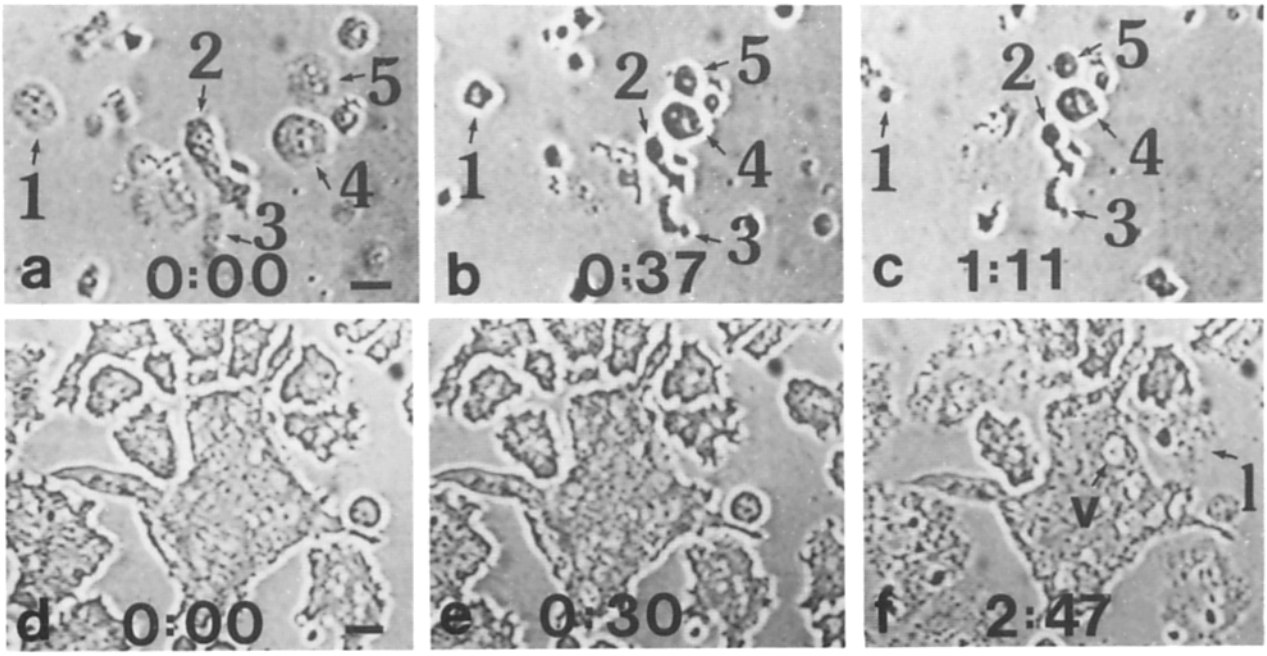


*Figure 10.* Video microscopy of Triton-permeabilized cell models of AX4 and *hmm* cells. (*a–c*) Sequential video frames showing the contraction of AX4 cells after addition of Mg-ATP. The numbers (1–5) refer to five representative cells located in these frames. (*d–f*) response of *hmm* cells. The numbers at the bottom indicate minutes and seconds. *v* (*f*): vacuole. *l* (*f*): lysed cell. Bar, 5 μm. ×1,000.

or morphological polarity and extend lamellipodia and pseudopodia in nearly random directions. These structures included as much F-actin as wild-type cells, in the absence of conventional myosin. Although the mechanism of how actin is assembled and incorporated into newly forming cell processes is unknown, our results suggest that the extension of cellular projections do not require the motive force generated by the conventional myosin. It is possible that these functions are primarily dependent on actin-based structural changes in association with specific binding proteins. For example, it has been demonstrated that *Dictyostelium* 120- (4, 10) and 30-kD (16) actin binding proteins are selectively localized in new actin-filled projections or filopodia respectively. It is also possible that another class of myosin (11, 21) may be involved in these activities.

It should be noted that a significant amount of F-actin was observed in the "pseudo-cleavage furrow". Recent studies using high-resolution polarized light and immunofluorescence microscopies showed that there is a unique array of actin bundles at the cleavage furrow in the wild type (19). This actin array is organized parallel to the polar axis, perpendicular to the contractile ring, and is not associated with myosin. Whether this actin organization occurs in the *hmm* cells and the role of this actin in cell division remain to be determined. Importantly, in most cases, *hmm* cells fail to complete division by forming pseudo-cleavage furrows. This evidence is consistent with a long-believed idea that myosin is essential for cytokinesis (17, 34, 45). This and previous studies (12, 32, 35) provide direct evidence for the necessity of conventional myosin for cytokinesis.

### *Response of hmm Cells to cAMP*

Our studies showed that *hmm* cells respond to cAMP and are induced to form surface blebs. Although this response occurred slower than the "cringing" of the wild type (~25 s, reference 24), the blebbing seems to be one of the typical behavioral responses induced with cAMP. Dr. Fontana and Dr. Devreotes found that pseudopodia were extended in all directions ~15–30 s after cAMP stimulation (reference 5, p.229). More recently, we have confirmed the temporal formation of similar surface blebs, and also showed localized actin and myosin in these structures (36).

There was, however, a significant difference in the cAMP-stimulation response between *hmm* and wild-type cells. The *hmm* cells became irregular and did not round up after stimulation with cAMP. The results suggest that the cAMP-elicited blebbing can be induced without the presence of conventional myosin, and might be due to a local polymerization of actin and/or the presence of actin-binding protein(s). On the other hand, it is obvious that the rounding up of the cell requires the normal organization of conventional myosin.

### *Contraction of hmm Cells*

The inability of *hmm* cells to cap Con-A receptors suggests that the conventional myosin is prerequisite for lateral mobility of surface receptors. The inability of *hmm* cells to contract their cortical cytoskeleton was further demonstrated with Triton-insoluble cytoskeletons of *hmm* cells. Although the nature of the dramatically reduced level of surface tension maintained by *hmm* cells (40) and the mechanism of altered cell motility of this mutant are unknown, this study demonstrated that the conventional myosin is crucial in constricting major cortical cytoskeletons.

This work was supported by National Institutes of Health (NIH) grants GM-39548 and RR-05370 to Y. Fukui; American Cancer Society, Illinois Division Inc., Research grant no. 87-24 to Y. Fukui; and NIH grant GM-40509 to J. Spudich.

Received for publication 19 May 1989 and in revised form 24 October 1989.

## References


1. Berlot, C. H., P. N. Devreotes, and J. A. Spudich. 1987. Chemoattractant-elicited increases in *Dictyostelium* myosin phosphorylation are due to changes in myosin localization and increases in kinase activity. *J. Biol. Chem.* 262:3918–3926.
2. Bonner, J. T. 1947. Evidence for the formation of cell aggregates by chemotaxis in the development of the slime mold *Dictyostelium discoideum*. *J. Exp. Zool.* 106:1–26.
3. Bonner, J. T. 1969. Hormones in social amoebae and mammals. *Sci. Am.* 220:78–91.
4. Carboni, J. M., and J. S. Condeelis. 1985. Ligand-induced changes in the location of actin, myosin, 95K (α-actinin), and 120K protein in amebae of *Dictyostelium discoideum*. *J. Cell Biol.* 100:1884–1893.
5. Chisholm, R. L., D. Fontana, A. Theibert, H. F. Lodish, and P. Devreotes. 1985. Development of *Dictyostelium discoideum*: chemotaxis, cell-cell adhesion, and gene expression. *In* Microbial Development. R. Losick and L. Shapiro, editors. Cold Spring Harbor Laboratory, Cold Spring Harbor, NY. 219–254.
6. Clarke, M., and J. A. Spudich. 1974. Biochemical and structural studies of actomyosin-like proteins from non-muscle cells. Isolation and characterization of myosin from amoebae of *Dictyostelium discoideum*. *J. Mol. Biol.* 86:209–222.
7. Clarke, M., and J. A. Spudich. 1977. Nonmuscle contractile proteins: The role of actin and myosin in cell motility and shape determination. *Annu. Rev. Biochem.* 46:797–822.
8. Cocucci, S., and M. Sussman. 1970. RNA in cytoplasmic and nuclear fractions of cellular slime mold amebas. *J. Cell Biol.* 45:399–407.
9. Collins, J. H., G. P. Côté, and E. D. Korn. 1982. Localization of the three phosphorylation sites on each heavy chain of *Acanthamoeba* myosin II to a segment at the end of the tail. *J. Biol. Chem.* 257:4529–4534.
10. Condeelis, J. 1983. Rheological properties of cytoplasm: Significance for the organization of spatial information and movement. *Modern Cell Biol.* 2:225–240.
11. Côté, P. G., J. P. Albanesi, T. Ueno, J. A. Hammer, III, and E. D. Korn. 1985. Purification from *Dictyostelium discoideum* of a low-molecular-weight myosin that resembles myosin I from *Acanthamoeba castellanii*. *J. Biol. Chem.* 260:4543–4546.
12. De Lozanne, A., and J. A. Spudich. 1987. Disruption of the *Dictyostelium* myosin heavy chain gene by homologous recombination. *Science (Wash. DC).* 236:1086–1091.
13. De Lozanne, A., M. Lewis, J. A. Spudich, and L. A. Leinwand. 1985. Cloning and characterization of a nonmuscle myosin heavy chain cDNA. *Proc. Natl. Acad. Sci. USA.* 82:6807–6810.
14. De Lozanne, A., C. H. Berlot, L. A. Leinwand, and J. A. Spudich. 1987. Expression in *Escherichia coli* of a functional *Dictyostelium* myosin tail fragment. *J. Cell Biol.* 105:2999–3005.
15. De Lozanne, A., H. M. Warrick, R. Chasan, L. A. Leinwand, and J. A. Spudich. 1988. Molecular genetic approaches to myosin function. *In* Signal Transduction in Cytoplasmic Organization and Cell Motility. P. S. and J. S. Condeelis, editors. Alan R. Liss, Inc., NY. 279–286.
16. Fechheimer, M. 1987. The *Dictyostelium discoideum* 30,000-dalton protein is an actin filament-bundling protein that is selectively present in filopodia. *J. Cell Biol.* 104:1539–1551.
17. Fujiwara, K., and T. D. Pollard. 1976. Fluorescent antibody localization of myosin in the cytoplasm, cleavage furrow and mitotic spindle of human cells. *J. Cell Biol.* 71:847–875.
18. Fukui, Y. 1980. Formation of multinuclear cells induced by dimethyl sulfoxide: inhibition of cytokinesis and occurrence of novel nuclear division in *Dictyostelium* cells. *J. Cell Biol.* 86:181–189.
19. Fukui, Y. 1990. Actomyosin organization in mitotic *Dictyostelium* amoebae. *Ann. NY Acad. Sci.* In press.
20. Fukui, Y., and S. Yumura. 1986. Actomyosin dynamics in chemotactic amoeboid movement of *Dictyostelium*. *Cell Motil. Cytoskel.* 6:662–673.
21. Fukui, Y., T. J. Lynch, H. Brzeska, and E. D. Korn. 1989. Myosin I is located at the leading edges of locomoting *Dictyostelium* amoebae. *Nature (Lond.).* 341:328–331.
22. Fukui, Y., S., Yumura, T. K. Yumura, and H. Mori. 1986. Agar overlay method: high-resolution immunofluorescence for the study of the contractile apparatus. *Methods Enzymol.* 134:573–580.
23. Fukui, Y., S. Yumura, T. K. Yumura. 1987. Agar-overlay immunofluorescence: high-resolution studies of cytoskeletal components and their changes during chemotaxis. *Methods Cell Biol.* 28:347–356.
24. Futrell, R. P., J. Traut, and W. G. McKee. 1982. Cell behavior in *Dictyostelium discoideum*: Preaggregation response to localized cyclic AMP pulses. *J. Cell Biol.* 92:807–821.
25. Gerisch, G., and B. Hess. 1974. Cyclic-AMP-controlled oscillations in suspended *Dictyostelium* cells: their relation to morphogenetic cell interactions. *Proc. Natl. Acad. Sci. USA.* 71:2118–2122.
26. Griffith, L. M., S. M. Downs, and J. A. Spudich. 1987. Myosin light chain kinase and myosin light chain phosphatase from *Dictyostelium*: effects of reversible phosphorylation on myosin structure and function. *J. Cell Biol.* 104:1309–1323.
27. Kay, R. 1987. Gene targeting in *Dictyostelium*: what do cells need myosin for? *Trends Genet.* 3:174–175.
28. Kiehart, D. P., and T. D. Pollard. 1984. Stimulation of *Acanthamoeba* actomyosin ATPase activity by myosin-II polymerization. *Nature (Lond.).* 308:864–866.
29. Kitanishi-Yumura, T., and Y. Fukui. 1987. Reorganization of microtubules during mitosis in *Dictyostelium*: dissociation from MTOC and selective assembly/disassembly *in situ*. *Cell Motil. Cytoskel.* 8:106–117.
30. Kitanishi-Yumura, T., and Y. Fukui. 1989. Actomyosin organization during cytokinesis: reversible translocation and differential redistribution in *Dictyostelium*. *Cell Motil. Cytoskel.* 12:78–89.
31. Kitanishi-Yumura, T., S. H. Blose, and Y. Fukui. 1985. Role of the MT-MTOC complex in determination of the cellular locomotory unit in *Dictyostelium*. *Protoplasma.* 127:133–146.
32. Knecht, D. A., and W. F. Loomis. 1987. Antisense RNA inactivation of myosin heavy chain gene expression in *Dictyostelium discoideum*. *Science (Wash. DC).* 236:1081–1086.
33. Kuczmarski, E. R., and J. A. Spudich. 1980. Regulation of myosin self-assembly: phosphorylation of *Dictyostelium* heavy chain inhibits formation of thick filaments. *Proc. Natl. Acad. Sci. USA.* 77:7292–7296.
34. Mabuchi, I., and M. Okuno. 1977. The effect of myosin antibody on the division of starfish blastomeres. *J. Cell Biol.* 74:251–263.
35. Manstein, D. J., M. A. Titus, A. De Lozanne, and J. A. Spudich. 1989. Gene replacement in *Dictyostelium*: generation of myosin null mutants. *EMBO (Eur. Mol. Biol. Organ.) J.* 8:923–932.
36. Nachmias, V., Y. Fukui, and J. A. Spudich. 1989. Chemoattractant-elicited translocation of myosin in motile *Dictyostelium*. *Cell Motil. Cytoskel.* 13:158–169.
37. Omura, F., and Y. Fukui. 1985. *Dictyostelium* MTOC: Structure and linkage to the nucleus. *Protoplasma.* 127:212–221.
38. Page, K., H. Maruta, M. Claviez, and G. Gerisch. 1984. Localization of two phosphorylation sites adjacent to a region important for polymerization on the tail of *Dictyostelium* myosin. *EMBO (Eur. Mol. Biol. Organ.) J.* 3:3271–3278.
39. Pasternak, C., P. F. Flicker, S. Ravid, and J. A. Spudich. 1989. Intermolecular and intramolecular interactions of *Dictyostelium* myosin: possible regulation by heavy chain phosphorylation. *J. Cell Biol.* 109:203–210.
40. Pasternak, C., J. A. Spudich, and E. L. Elson. 1989. Capping surface receptors and concomitant cortical tension are generated by conventional myosin. *Nature (Lond.).* 341:549–551.
41. Peltz, G., J. A. Spudich, and P. Parham. 1985. Monoclonal antibodies against several sites on the head and tail of *Dictyostelium* myosin. *J. Cell Biol.* 100:1016–1023.
42. Pollard, T. D., and E. D. Korn. 1973. *Acanthamoeba* myosin. I. Isolation from *Acanthamoeba castellanii* of an enzyme similar to muscle myosin. *J. Biol. Chem.* 248:4682–4690.
43. Pollard, T. D., and E. D. Korn. 1973. *Acanthamoeba* myosin. II. Interaction with actin and with a new cofactor protein required for actin activation of $Mg^{2+}$ adenosine triphosphate activity. *J. Biol. Chem.* 248:4691–4697.
44. Reines, D., and M. Clarke. 1985. Immunochemical analysis of the supramolecular structure of myosin in contractile cytoskeletons of *Dictyostelium* amoebae. *J. Biol. Chem.* 260:14248–14254.
45. Schroeder, T. E. 1987. Fourth cleavage of sea urchin blastomeres: microtubule patterns and myosin localization in equal and unequal cell divisions. *Dev. Biol.* 124:9–22.
46. Sheetz, M., and J. A. Spudich. 1983. Movement of myosin-coated fluorescent beads on actin cables *in vivo*. *Nature (Lond.).* 303:31–35.
47. Singer, S. J., J. A. Ash, L. Y. W. Bourguignon, M. H. Heggeness, and D. Louvard. 1978. Transmembrane interactions and the mechanisms of transport of proteins across membranes. *J. Spramol. Struct.* 9:373–389.
48. Solomon, F. 1987. What myosin might do? *Science (Wash. DC).* 236:1043–1044.
49. Spudich, J. A., and A. Spudich. 1982. Cell motility. *In* The Development of Dictyostelium discoideum. W. F. Loomis, editor. Academic Press, NY. 169–194.
50. Stendahl, O., J. H. Hartwig, E. A. Brotschi, and T. P. Stossel. 1980. Distribution of actin-binding protein and myosin in macrophages during spreading and phagocytosis. *J. Cell Biol.* 84:215–224.
51. Warrick, H. M., and J. A. Spudich. 1987. Myosin structure and function in cell motility. *Annu. Rev. Cell Biol.* 3:379–421.
52. Warrick, H. M., A. De Lozanne, L. A. Leinwand, and J. A. Spudich. 1986. Conserved protein domains in a myosin heavy chain gene from *Dictyostelium discoideum*. *Proc. Natl. Acad. Sci. USA.* 83:9433–9437.
53. Wessels, D., D. R. Soll, D. Knecht, W. F. Loomis, A. De Lozanne, and J. A. Spudich. 1988. Cell motility and chemotaxis in *Dictyostelium* amebae lacking myosin heavy chain. *Dev. Biol.* 128:164–177.
54. Yumura, S., and Y. Fukui. 1983. Filopodelike projections induced with dimethyl sulfoxide and their relevance to cellular polarity in *Dictyostelium*. *J. Cell Biol.* 96:857–865.
55. Yumura, S., and Y. Fukui. 1985. Reversible cyclic AMP-dependent change in distribution of myosin thick filaments in *Dictyostelium*. *Nature (Lond.).* 314:194–196.
56. Yumura, S., H. Mori, and Y. Fukui. 1984. Localization of actin and myosin for the study of ameboid movement in *Dictyostelium* using improved immunofluorescence. *J. Cell Biol.* 99:894–899.